

## FEATURE ARTICLE

## Vibrational Energy Transfer Modeling of Nonequilibrium Polyatomic Reaction Systems

John R. Barker,<sup>\*,†,‡</sup> Laurie M. Yoder,<sup>‡</sup> and Keith D. King<sup>\*,§</sup>

Department of Atmospheric, Oceanic, and Space Sciences, and Department of Chemistry, University of Michigan, Ann Arbor, Michigan 48109-2143, and Department of Chemical Engineering, Adelaide University, Adelaide, S.A., Australia, 5005

Received: June 8, 2000; In Final Form: November 8, 2000

The use of energy transfer data and models in describing nonequilibrium polyatomic reaction systems is discussed with particular emphasis on the information needed for modeling vibrational energy transfer. In the discussion, it is pointed out that key areas of energy transfer knowledge are still lacking and the available experimental data are limited in scope and are of uneven quality. Despite these limitations, it is still possible to carry out meaningful simulations of chemical systems in which vibrational energy transfer is important. The vibrational energy master equation, which is the basis for modeling, and various experiments and calculations that provide the basis for practical energy transfer models and parametrizations are described. Two examples of gas phase reaction systems are presented in which vibrational energy transfer is important. The decomposition of norbornene shows how energy transfer parameters can be obtained from measurements of shock-induced chemical reactions, but even the best such experiments provide only limited information about energy transfer. Chemically activated 2-methylhexyl radicals illustrate the complex reactions of multiple isomers connected by multiple isomerization pathways and reacting according to multiple decomposition pathways.

## Introduction

Nonequilibrium polyatomic reaction systems are governed by competition between chemical reaction and collisional energy transfer. It is this interplay that results in collisional energy transfer having a large influence on many chemical systems, e.g., laser-induced chemistry, pyrolysis, combustion, and atmospheric chemical processes. However, a full quantitative understanding of collisional energy transfer remains incomplete, especially for highly excited large polyatomic molecules.<sup>1</sup> This means that a full description of a nonequilibrium polyatomic reaction system requires the use of energy transfer data and models. Individual systems must be modeled not only to describe the experiments but also to make predictions when a reaction in question is occurring as part of a more complex system under experimental conditions far removed from those where limited measurements were obtained.

The promise of computer models is that they can predict the behavior of physicochemical systems that are so incredibly complex, or under such extreme conditions that conventional laboratory experiments are impractical. Electronic structure calculations are now routine. It is possible to calculate the relevant chemical structures, vibrational frequencies, moments of inertia, and chemical energies with useful accuracy. This information can be used with existing computer software to

predict physical properties and chemical characteristics (e.g., heats of reaction and transition-state theory rate constants<sup>2</sup>). All of this can be used to construct large models of complex gas phase physicochemical systems, such as combustion and atmospheric photooxidation. A current weak link in constructing predictive models that include large molecules is that energy transfer information is scarce.

Over the last several decades, considerable progress has been made in characterizing large molecule vibrational energy transfer (VET),<sup>3–7</sup> but it is not yet well understood on a fundamental basis. Much of what is known is descriptive, rather than predictive, and fragmentary, rather than complete. Yet it is still possible to construct reasonably detailed models of important reaction systems. Much of the work along these lines has been directed toward simulating or analyzing laboratory experiments that were designed from the start to probe large molecule energy transfer. More recently, the growth of computer modeling capabilities has encouraged predictive modeling of complex reactive systems.

In this paper, we place particular emphasis on the information needed for modeling chemical systems that involve VET. In the next section, we describe the vibrational energy master equation, which is the basis for modeling and which requires information about collisional energy transfer. In the following sections of the paper, we describe various experiments and calculations that provide the basis for practical energy transfer models and parametrizations. We then present two examples of gas phase reactions systems in which VET is important. The first example<sup>8</sup> shows how energy transfer parameters can be obtained from measurements of shock-induced chemical reac-

\* Address correspondence to these authors.

† Department of Atmospheric, Oceanic, and Space Sciences, University of Michigan.

‡ Department of Chemistry, University of Michigan.

§ Adelaide University.

tions, but even the best experimental shock tube data provides only fragmentary information about energy transfer. The second example is a complex chemical activation system that is typical of those found in hydrocarbon combustion and photooxidation. The results presented for this example constitute a *prediction*, since they are based entirely on calculations<sup>9</sup> that have not been verified by experiments. In the concluding section of the paper, we briefly discuss some of the key areas of knowledge that are still lacking.

### Master Equation for Vibrational Energy Transfer

The master equation provides the fundamental theoretical basis for modeling systems in which both energy transfer and chemical reaction can occur.<sup>10–13</sup> It comprises a set of coupled differential equations that describe the rates of production and loss of chemical species in specified energy states. In this paper, we will deal only with unimolecular reactions, but the basic concepts are easily extended to much more complex systems, which may include bimolecular reactions, laser-induced transitions, etc. We will confine our discussion to VET and the “one-dimensional” master equation, in which vibrational energy is modeled explicitly, while angular momentum is either neglected or treated only approximately. Extensions that explicitly include angular momentum (the two-dimensional master equation<sup>14–22</sup>) are beyond the scope of this paper. Trajectory calculations indicate that rotational energy transfer is much less important than VET in chemical systems that do not include barrierless reactions. The emphasis throughout this paper is placed on the collisional energy transfer aspects of modeling. Complementary discussions of energy-dependent unimolecular rate constants can be found elsewhere.<sup>10–12,23</sup> In the following subsections, the master equation is presented along with mention of pragmatic approximations and simplifications.

**Essentials.** At high vibrational energies, a quasicontinuum of vibrational states exists and intramolecular vibrational redistribution (IVR) is rapid. Experiments show that IVR is slow at low energy, exhibits multiple time scales, and becomes rapid at energies where the vibrational state density is of the order of  $10^2$ – $10^3$  states/cm<sup>-1</sup>.<sup>24</sup> At these state densities, some vibrational states overlap significantly within their natural widths as governed by infrared spontaneous emission rates. At state densities greater than  $\sim 10^7$  states/cm<sup>-1</sup>, most states are overlapped within their natural widths. The onset of rapid IVR is a convenient marker for the onset of the vibrational quasicontinuum (however, IVR exhibits multiple time constants and thus some modes remain isolated even at higher vibrational state densities<sup>24</sup>). In the vibrational quasicontinuum, individual quantum states cannot be resolved and the master equation can be written:

$$\frac{dy(E',t)}{dt} dE' = f(E',t) dE' + \int_0^\infty dE [R(E',E) dE' y(E,t)] - \int_0^\infty dE [R(E,E') dE' y(E',t)] - \sum_{m=1}^{\text{channels}} k_m(E') y(E',t) dE' \quad (1)$$

where  $y(E',t) dE'$  is the concentration of species with vibrational energy in the range  $E'$  to  $E' + dE'$ ,  $R(E,E')$  is the (pseudo-first-order) rate coefficient for VET from energy  $E'$  to energy  $E$ ,  $f(E',t) dE'$  is a source term (e.g., chemical or photo activation), and  $k_m(E')$  is a unimolecular reaction rate constant for molecules at energy  $E'$  reacting via the  $m$ th channel. Terms involving radiative emission and absorption have been omitted.

If the rate coefficients  $R(E,E')$  do not depend on the initial quantum states of the collider bath molecules, they can be written as the product of the *total vibrationally inelastic* collision frequency,  $\omega$  multiplied by the “collision step-size distribution”,  $P(E,E')$ , which expresses the probability that a molecule initially in the energy range from  $E'$  to  $E' + dE'$  will undergo an inelastic transition to the energy range  $E$  to  $E + dE$ :

$$R(E,E') dE = \int_0^\infty R(E,E') dE \left\{ \frac{R(E,E') dE}{\int_0^\infty R(E,E') dE} \right\} \quad (2a)$$

$$= \omega P(E,E') dE \quad (2b)$$

where the first factor on the rhs of eq 2a, the integral over the rates of all inelastic transitions from initial energy  $E'$ , is the frequency of inelastic collisions,  $\omega$ . The second factor on the rhs of eq 2a is the collision step-size distribution  $P(E,E')$ . Usually, the collision frequency is actually calculated from the expression  $\omega = k_{\text{coll}}[M]$ , where  $k_{\text{coll}}$  is the bimolecular rate constant for inelastic collisions (and in general may depend on  $E$ ) and  $[M]$  is the bath gas concentration. It is important to emphasize that the factorization of  $R(E,E')$  in eq 2 is merely for convenience and that  $k_{\text{coll}}$  and  $P(E,E')$  never occur independently of one another. Thus, the specific choice of a value for  $k_{\text{coll}}$  is tied to the expression for  $P(E,E')$ , since the product of the two must be independent of arbitrary choices. Furthermore,  $P(E,E')$  is only a proper probability density function when  $\omega$  is exactly equal to the inelastic collision rate constant. Under this assumption,  $P(E,E')$  is normalized:

$$\int_0^\infty P(E,E') dE = 1 \quad (3)$$

For the Lennard-Jones potential,  $k_{\text{coll}}$  takes the following form:<sup>3</sup>

$$k_{\text{coll}} = \pi \sigma^2 \langle v \rangle \Omega^{(2,2)*} \quad (4)$$

where  $\langle v \rangle$  is the average speed,  $\sigma$  is the Lennard-Jones diameter, and  $\Omega^{(2,2)*}$  is the collision integral, which depends on the Lennard-Jones parameters. Since only the product  $k_{\text{coll}} P(E,E')$  appears in the master equation, if  $k_{\text{coll}}$  is underestimated, then normalization of the step-size distribution is not appropriate. If, on the other hand,  $k_{\text{coll}}$  is overestimated, then  $P(E,E')$  must include elastic collisions. The inclusion of elastic collisions in the master equation causes no problems, except to reduce the efficiency of certain numerical techniques.

In a state-to-state experimental study using single vibrational level fluorescence, Lawrance and Knight<sup>25</sup> found that the observed total cross sections for inelastic collisions are in quantitative agreement with the Lennard-Jones collision frequency for a moderately high density of vibrational states. Classical trajectory calculations also support this assumption,<sup>26,27</sup> but the argument is somewhat circular in this case since the assumed potential energy functions are often constructed from pairwise Lennard-Jones potentials. Recently, Xue et al. found that the inelastic cross section for energy transfer from a single highly excited vibrational state in SO<sub>2</sub> is substantially *greater* than the Lennard-Jones cross section.<sup>28</sup> At low vibrational energies, however, it is well-known that the inelastic collision cross section is small<sup>29</sup> and thus the total inelastic collision rate constant is probably smaller than  $k_{\text{LJ}}$ . In any event, the quantum total cross section<sup>30</sup> provides a rigorous upper limit to  $k_{\text{coll}}$ .

With these substitutions, the master equation can be written:

$$\frac{dy(E',t)}{dt}dE' = f(E',t) dE' + \omega \int_0^\infty dE [P(E',E) dE' y(E,t)] - \omega y(E',t) dE' - \sum_{m=1}^{\text{channels}} k_m(E') y(E',t) dE' \quad (5)$$

Note that the rates of activating and deactivating collisions are connected via detailed balance:

$$\frac{P(E,E')}{P(E',E)} = \frac{\rho(E)}{\rho(E')} \exp\left\{-\frac{E-E'}{k_B T}\right\} \quad (6)$$

where  $\rho(E)$  is the density of states at energy  $E$  and  $k_B$  is the Boltzmann constant. In many applications, eq 5 is solved numerically by approximating it with finite differences.<sup>3,12</sup> An alternative method of solution that does not require energy graining at high energies is based on a stochastic representation, as described elsewhere.<sup>13,31,32</sup> Several public domain computer codes are available for solving the master equation.<sup>2,32,33</sup> At low and intermediate energies, there are wide energy gaps between adjacent vibrational states and  $P(E,E')$  cannot be approximated accurately as a continuous function. This sparse density of states regime persists to relatively high energies in small “stiff” molecules (e.g.,  $\sim 2000 \text{ cm}^{-1}$  in benzene<sup>34</sup>), but only to relatively low energies in large, floppy molecules (e.g.,  $\sim 500 \text{ cm}^{-1}$  in 2-methylhexyl radicals<sup>9</sup>). In an energy-grained master equation, the step-size distribution need not be a continuous function and can be set equal to zero in grains which do not contain states. The public domain code MultiWell<sup>32,34</sup> and its predecessors<sup>8,13</sup> were designed to accommodate the sparse density of states regime with discontinuous  $P(E,E')$  at low energy, as well as the quasicontinuum at high energy.

**Additional Terms.** The following phenomena are common in nonequilibrium chemical systems and necessitate the inclusion of additional terms on the rhs of eq 5.

*Infrared Emission and Absorption.* At low pressures, spontaneous radiative emission provides the deactivation process that enables radiative recombination reactions.<sup>35,36</sup> Spontaneous infrared emission contributes a source term and a loss term to the master equation, and similar terms can be written for other types of radiative emission.<sup>37,38</sup> These expressions can be generalized for multiphoton transitions.<sup>39,40</sup>

*V–V Energy Transfer.* V–V energy transfer is important in a number of chemical systems.<sup>41,42</sup> The master equation for V–V energy transfer consists of more than just adding a few additional terms to eq 5. The equation must be modified to reflect the effects of the internal energy of the collision partner and a second set of coupled equations must be added in order to describe the time dependence of the collision partner internal energy. To the best of our knowledge, nonlinear master equations of this type have not yet been used in modeling studies of polyatomic reaction systems, although detailed energy transfer information is now becoming available.<sup>7,43–47</sup>

### Energy Transfer Models

The energy transfer information necessary for one-dimensional linear master equation simulations is contained in  $P(E,E')$  and in  $k_{\text{coll}}$ . Information about these quantities varies in source and in quality.

**State-to-State Rate Constants.** Experimental state-to-state data on V–T energy transfer have been obtained both in thermal gas phase systems and in molecular beams using molecules excited within the sparse density of states regime. In general,

energy transfer in this regime is characterized by complicated quantum interference effects due to coupled states.<sup>48</sup> The data show that some vibrational modes exhibit a propensity to transfer energy very readily, compared to other vibrational modes. These experiments have produced a wealth of detailed energy transfer information.<sup>7,49,50</sup> For the present discussion, the most important conclusions from the state-to-state experiments are that (a) the VET propensities persist in the sparse density of states regime, and (b) the data on aromatic molecules can be described semiquantitatively with SSH(T) theory,<sup>51</sup> the “breathing sphere” extension to polyatomics of the venerable SSH theory,<sup>52,53</sup> which was originally developed for diatomic VET.

Several theoretical techniques exist for accurately calculating state-to-state rate constants for low-lying vibrational states. In particular, Clary and co-workers<sup>54,55</sup> have reported VCC–IOS (vibrationally close coupled, infinite order sudden approximation) calculations of rate constants for transitions among the lowest states of several polyatomic molecules in collisions with monatomic gases. Although powerful, this method is computationally intensive and can be extended to higher-lying states only with difficulty.<sup>56</sup> Nonetheless, the VCC–IOS results give direct information about the inelastic energy transfer rates  $R_{ij}$  and, hence,  $P(E,E')$ .

**Energy- and Temperature-Dependent  $\langle \Delta E \rangle$ .** *Experiments.* Traditionally, polyatomic VET was measured near reaction thresholds in thermal and chemical activation unimolecular reaction studies. Those pioneering studies were affected by broad internal energy distributions (in thermal studies) and complications due to complex chemical reaction systems. Nonetheless, the relative rate constants obtained for VET clearly showed that the energy transfer effectiveness depends on the number of atoms of the bath gas molecule.<sup>3–5</sup> The relative values for many bath gases were shown to be almost independent of the particular reaction system under investigation. By using chemical activation, which produces relatively narrow internal energy distributions, Rabinovitch and co-workers showed that the “exponential” step-size distribution gave better simulations of data for monatomic bath gases, while the “step-ladder” distribution gave better simulations for polyatomic bath gases, and there were hints that the energy transfer efficiencies might depend on vibrational energy.<sup>3</sup> The mathematically convenient exponential model is written in terms of deactivation collisions:

$$P(E,E') = \frac{1}{N(E')} \exp\left\{-\frac{E'-E}{\alpha}\right\}, \quad \text{for } E' > E \quad (7)$$

where  $N(E')$  is the normalization constant and  $\alpha$  is a parameter that may depend on energy (the corresponding expression for the activation collisions is obtained from detailed balance<sup>3–5</sup>). The parameter  $\alpha$  is closely related to the average energy transferred in deactivating collisions,  $\langle \Delta E(E') \rangle_d$ , which is convenient for summarizing the energy transfer effectiveness:

$$\langle \Delta E(E') \rangle_d = \frac{\int_0^{E'} (E' - E) P(E,E') dE}{\int_0^{E'} P(E,E') dE} \quad (8)$$

Note that  $\langle \Delta E(E') \rangle_d$  differs from  $\langle \Delta E(E') \rangle_{\text{all}}$ , a second measure of energy transfer effectiveness, in that for the latter quantity the sign of the expression is reversed and the upper integration limits are extended to  $\infty$ . Note that  $\langle \Delta E(E') \rangle_{\text{all}}$  includes the temperature dependence associated with activation collisions (eq 6).

About 20 years ago, two techniques came into vogue for studying energy transfer involving highly vibrationally excited

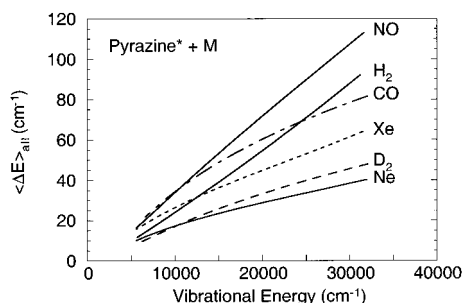


**Figure 1.** Average energies transferred per collision as a function of vibrational energy for excited pyrazine deactivated by various colliders at 300 K.

**TABLE 1: Recommended Data for  $\langle \Delta E \rangle_d$  or  $\langle \Delta E \rangle_{\text{all}}$**

excited species	notes	accuracy <sup>a</sup>	references
azulene	IRF, 300 K	b	152
	IRF, 300–600 K	b	75
	UVA, 300–800 K	c	153
	KCSI	a	60, 65
benzene	IRF	b	117
biphenylene	UVA, 333–523 K	a	66
cycloheptatriene derivatives	UVA, T-dependence	c	80
hexafluorobenzene	UVA	c	74
	IRF	b	71, 72
norbornene	modeling of shock tube data, 300–1500 K	c	8
pyrazine ( $S_0$ )	IRF, 300 K	b	62
	IRF, 254–414 K	b	76
toluene	IRF	b	117
	UVA, T-dependence	c	80, 154
	KCSI	a	60, 61, 65
relative values for many excited species and colliders	UVA	d	5, 155
	unimolecular/recombination reactions	d	3–5

<sup>a</sup> Roughly estimated maximum relative uncertainties in  $\langle \Delta E \rangle_{\text{all}}$  or  $\langle \Delta E \rangle_d$ : a, 5–10%; b, 20–30%; c, 30–50%; d, 10% for relative  $\langle \Delta E \rangle$  values.

polyatomics in the electronic ground state.<sup>5</sup> These techniques do not rely on chemical reactions, but instead are based on time-resolved spontaneous infrared fluorescence (IRF)<sup>57</sup> and on ultraviolet absorbance (UVA),<sup>58</sup> respectively. Other techniques based on physical properties were also investigated at about the same time (e.g., time-dependent thermal lensing (TDTL)<sup>59</sup>), but they were not as generally useful. Neither technique is sensitive to rotations and thus the results are confined to VET. Both the IRF and UVA techniques produced relative rates of VET at high energies in good agreement with the earlier unimolecular reaction studies and absolute values in reasonable agreement with each other. The IRF technique also revealed that the average vibrational energy transferred per collision depends almost linearly on the vibrational energy. (Early measurements using the UVA technique did not show this energy dependence, possibly due to calibration errors,<sup>60,61</sup> but later work is in general agreement with the IRF results.) Some recent results<sup>62</sup> obtained using the IRF technique are presented in Figure 1, where the nearly linear energy dependence is apparent. Example systems that have been investigated using the IRF and UVA techniques are summarized in Table 1.

The most accurate energy transfer information currently available for large molecules has been obtained by Luther and co-workers with the kinetically controlled selective ionization

(KCSI) technique.<sup>61,63–65</sup> In conjunction with modeling, this technique has confirmed the vibrational energy dependence of the energy transfer rate constants first shown by the IRF technique and has produced results which are very precise and agree with the earlier IRF and UVA results to within 20%–50%.

The uncertainties in the IRF, UVA, and KCSI techniques depend on excitation energy. Moreover, the IRF and UVA techniques rely on theoretical and experimental calibration curves, respectively, which may have unrecognized systematic errors. The KCSI technique, in contrast, appears to be less susceptible to calibration errors. As a rough guide, the KCSI technique is reported to give  $\langle \Delta E \rangle$  values accurate to 5%–10% over the energy range up to about 40000 cm<sup>-1</sup>.<sup>60,61,65</sup> Based on our experience with the IRF technique and comparisons with KCSI results,<sup>60</sup> the IRF technique appears to be accurate to within about 20%–30% over the same energy range. The UVA technique is reported to have been subject to significant systematic calibration problems,<sup>60</sup> and we estimate that it is accurate to about 30%–50%, unless extra efforts are made to refine the calibration curves (e.g., see ref 66). Our estimates are very crude and ignore the energy dependence of  $\langle \Delta E \rangle$ , but they provide simple guidelines for the use of the data in Table 1: when available, KCSI data are preferred to the IRF data, which are preferred to the UVA data. When special efforts are made to assess the calibration curve uncertainties, the UVA accuracy can be improved to ~10%.<sup>66</sup> However, note that in all cases the *relative* values of  $\langle \Delta E \rangle$  are certainly much more accurate than the *absolute* values. Note also that the older unimolecular reaction data provide useful values for relative magnitudes of  $\langle \Delta E \rangle$ . These estimated uncertainties are indicated in Table 1.

Both the IRF and UVA techniques rely on UV excitation and subsequent fast radiationless transitions for production of vibrationally excited species in the electronic ground state. A very useful alternative method for producing highly vibrationally excited molecules in the electronic ground state is infrared multiphoton absorption (IRMPA).<sup>67–70</sup> Note that IRMPA is a more general technique, because it only relies on strong infrared absorption cross sections and not on the special photophysics needed for fast radiationless transitions. However, the vibrational energy distributions produced by IRMPA are difficult to characterize in detail. Recently, the first direct comparison between energy transfer parameters measured with IRMPA versus the standard IRF technique was carried out<sup>71,72</sup> using hexafluorobenzene, which has also been studied using the UVA method.<sup>73,74</sup> For deactivation by the series of noble gas colliders, the average energy transferred per collision was found to be essentially a linear function of energy and indistinguishable from the IRF results. This result gives confidence that the IRMPA method will produce good results in future studies.

Both the IRF and UVA techniques have shown that  $\langle \Delta E \rangle_d$  and  $\langle \Delta E \rangle_{\text{all}}$ , which are related via detailed balance (eq 6), depend only weakly on temperature. Equation 9 shows the approximate relationship between the two quantities (for more detail, see ref 75).

$$\langle \Delta E \rangle_{\text{all}} = k_B T - \langle \Delta E \rangle_d \quad (9)$$

We prefer to discuss  $\langle \Delta E \rangle_d$  instead of  $\langle \Delta E \rangle_{\text{all}}$  because the latter quantity includes a trivial thermodynamic contribution and the former quantity is more convenient for simulations. Some other workers prefer to discuss  $\langle \Delta E \rangle_{\text{all}}$ , because it is more easily extracted from measurements. This difference is an important point of potential confusion, and readers should remain aware

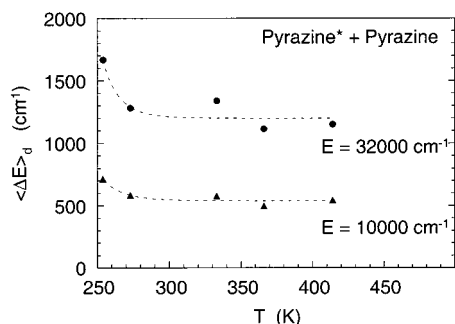


**Figure 2.** Average energies transferred per deactivating collision  $\langle \Delta E \rangle_d$  as functions of vibrational energy (10 000 and 32 000  $\text{cm}^{-1}$ ) and temperature for pyrazine self-deactivation (points). The dashed lines are intended only to guide the eye.

of it in the literature and in the following discussion. Also note that the collision frequency calculated from eq 4 includes an intrinsic temperature dependence that depends on the Lennard-Jones well depth.

Values of  $\langle \Delta E \rangle_d$  obtained as a function of temperature in a recent IRF investigation<sup>76</sup> of highly excited pyrazine deactivation in collisions with unexcited pyrazine are shown in Figure 2. Two IRF wavelengths were used in this investigation: the C–H stretch fundamental and its overtone at  $\sim 3040$  and  $\sim 6000 \text{ cm}^{-1}$ , respectively. The experiments were modeled with a master equation approach and it was found that the simple exponential model with energy-dependent parameter  $\alpha(E)$  could adequately simulate data obtained using each wavelength individually, but a biexponential model was necessary to simulate both sets of data simultaneously. Parameters for the biexponential model were obtained by fitting the time-dependent IRF intensities at each temperature and by assuming Lennard-Jones collisions. The values of  $\langle \Delta E \rangle_d$  extracted from this analysis differ, depending on whether one or two IRF wavelengths were used in the analysis. This difference produces different estimates of how the population distribution evolves with time at a given pressure and temperature, and the two-color analysis is preferred. However, both methods show that  $\langle \Delta E \rangle_d$  has very little temperature dependence, except at temperatures below 300 K, where V–V energy transfer<sup>77</sup> may be more significant. This low-temperature enhancement in  $\langle \Delta E \rangle_d$  has been reproduced in recent trajectory calculations, where it was ascribed to the shift in the position of the centrifugal barrier maximum to larger radii at low temperature.<sup>78</sup> This description is reminiscent of the models proposed by Parmenter and co-workers, who showed strong correlations between Lennard-Jones well depths and energy transfer probabilities.<sup>79</sup>

Previous IRF experiments using excited azulene deactivated by nitrogen or by unexcited azulene also showed virtually no variation from 300 K to  $\sim 600$  K.<sup>75</sup> Results from UVA experiments on  $\langle \Delta E \rangle_{\text{all}}$  over a wide range of temperatures also show only a weak temperature dependence, but these results are more difficult to assess since the vibrational energy dependence of  $\langle \Delta E \rangle_{\text{all}}$  was not detected.<sup>80</sup> A recent UVA study<sup>66</sup> of the temperature dependence of biphenylene energy transfer is consistent with the earlier results. All of the IRF and UVA results contrast with the recent experiments carried out using chemically activated alkyl free radicals.<sup>81–84</sup> In several cases, the chemical activation method produced  $\langle \Delta E \rangle_{\text{all}}$  values that are approximately directly proportional to temperature. The reasons for this difference are not known, although the use of chemical activation potentially introduces side reactions involving the free radicals. Furthermore, the alkyl free radicals are structurally quite different from the aromatics studied by IRF and UVA, perhaps

leading to different energy transfer behavior. The chemical activation results were analyzed without considering the likely energy dependence of  $\alpha(E, T)$ , but this oversight is not expected to affect the results significantly for single-channel reactions of small species.

Brown et al.<sup>85</sup> used a combination of thermal activation (the pressure-dependent very low pressure pyrolysis (VLPP) technique)<sup>86</sup> and infrared multiphoton decomposition (IRMPD) experiments<sup>67–70</sup> to investigate the temperature dependence of collisional energy transfer in ethyl acetate with the bath gases He, Ar, Ne, Kr, and  $\text{N}_2$ . This reaction system is very clean and free of chemical complications. It was found that  $\langle \Delta E \rangle_d$  is proportional to  $T^{-(0.1-0.3)}$  for He and Ne, and to  $T^{-(0.3-0.5)}$  for Ar, Kr, and  $\text{N}_2$  over the temperature range 340–850 K. Unlike the alkyl radical systems described above, the ethyl acetate system gave results quite similar to those measured in nonreactive systems via the IRF and UVA techniques.<sup>85</sup> Some modelers have assumed that  $\langle \Delta E \rangle_{\text{all}}$  is independent of temperature (and thus  $\langle \Delta E \rangle_d$  varies in a way that compensates for the increase of collisional activation steps with temperature). Others have assumed that  $\langle \Delta E \rangle_{\text{all}}$  (or  $\langle \Delta E \rangle_d$ ) is directly proportional to temperature. The uncertainty is serious, because of the wide temperature ranges that exist in many important chemical systems.

Experiments on the predissociation of van der Waals (vdW) dimers have been used to indirectly investigate VET.<sup>87,88</sup> Vibrational predissociation of a cluster, which is often termed a “half collision”, corresponds in some ways to a very low-temperature version of a full collision. Because of the weak temperature dependence of collisional energy transfer, the results on energy disposal in the cluster partners provide clues about energy transfer in collisions. The probability distributions for V–T energy transfer were found to be approximately exponential, and not highly sensitive to vibrational energy content. The energy transferred from vibrational modes of the molecule to rotation and translation of the partners is only a small fraction ( $< 3\%$ ) of the total vibrational energy, due to poor coupling between the high-frequency molecular modes and the low-frequency vdW modes. The energy transfer in cluster predissociation has been linked to collisional energy transfer using classical trajectory simulations.<sup>27</sup>

*Classical Trajectory Calculations.* Classical mechanics is the only theory which has so far proven to be generally useful for large molecule energy transfer.<sup>12,26,89–92</sup> Classical trajectory calculations provide considerable insight, but they must be viewed with caution.<sup>93,94</sup> Among other limitations, the total energy in a large molecule is rarely large enough, compared with the zero-point energy, to achieve the classical limit. Recent tests<sup>95</sup> have confirmed the expectation that classical and quantum mechanics give comparable results when the average excitation energy per mode is high, but that condition is rarely met for large molecules. For example, the average vibrational mode contains less than two quanta when benzene is excited to the C–H bond dissociation energy. Various methods have been proposed for forcing classical trajectory calculations to “conserve” zero-point energy, but none has been fully successful.<sup>96,97</sup> Furthermore, classical collision cross sections are infinite and several methods have been used with varying degrees of success for distinguishing elastic from inelastic collisions. The step-size distribution deduced from classical trajectories is usually described with a biexponential function, although Luther and co-workers have commented<sup>61,65,98</sup> that the second component of the distribution tends to be exaggerated, relative to experi-

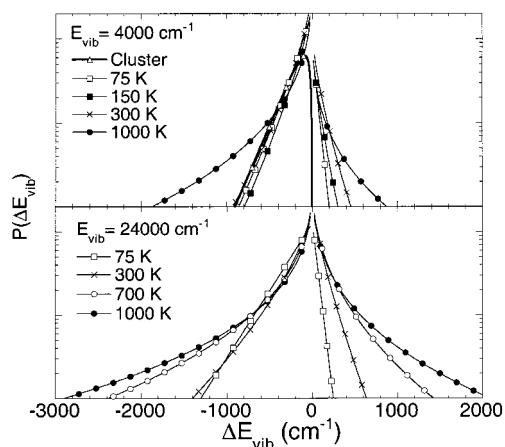


**Figure 3.** Calculated collision step-size probability histograms for pyrazine–Ar collisions as functions of (rotational and translational) temperature and initial vibrational energy (in addition to the zero-point energy). The elastic peaks are not shown. Each histogram is calculated from 30 000 trajectories.

mental measurements, unless the potential energy function is based on high-quality ab initio methods.<sup>99</sup>

At Michigan, trajectory calculations were carried out to simulate pyrazine–Ar vdW cluster vibrational predissociation (“half collisions”).<sup>27</sup> The intramolecular potential, which consisted of harmonic and Morse oscillators, was combined with a pairwise Lennard-Jones interaction potential. The calculated recoil distributions are in good agreement with the experimental data.<sup>87,88,100</sup> Using the same potential surface, “full collision” trajectories were computed for several temperatures and pyrazine initial internal energies. The calculated vibrational step-size histograms (10  $\text{cm}^{-1}$  bins) were least-squares fitted to the generalized exponential (eq 9) and are shown in Figure 3 for each temperature and for the cluster dissociation ( $V \rightarrow RT$  energy transfer). The probability for weak deactivating collisions ( $\Delta E < \sim 400 \text{ cm}^{-1}$ ) is nearly independent of temperature, and the slope of  $P(E, E')$  for cluster dissociation is nearly the same as that for the low-temperature ( $< 300 \text{ K}$ ) collisions. This result is noteworthy, because it suggests that vdW cluster dissociation experiments can be used to obtain collisional energy transfer information. However, the high-energy tail of the calculated step-size distribution is enhanced at higher temperatures, perhaps indicating that the energy transfer mechanism changes around 300 K (for this potential surface) and collisions that transfer very large energies (sometimes termed “supercollisions”<sup>101</sup>) become more probable. Trajectory calculations have been used by other groups to assess the temperature dependence of energy transfer and all agree that the temperature dependence is weak.<sup>102,103</sup> The very recent study published by Grigoleit et al.<sup>78</sup> reviews the earlier trajectory calculations, carries out a careful analysis of effects, and shows excellent agreement with some of the available experimental data.

**Complications. V–V Energy Transfer.** Poel et al.<sup>104–106</sup> have used the time-resolved IRF technique to study the vibrational deactivation of  $\text{CO}_2(00^01)$  and  $\text{N}_2\text{O}(00^01)$  by large polyatomic molecules (c- $\text{C}_6\text{H}_{10}$ , c- $\text{C}_6\text{H}_{12}$ ,  $\text{C}_6\text{H}_6$ ,  $\text{C}_6\text{D}_6$ ,  $\text{C}_7\text{H}_8$ ,  $\text{C}_7\text{D}_8$ ,  $\text{C}_6\text{H}_5\text{F}$ , p- $\text{C}_6\text{H}_4\text{F}_2$ ,  $\text{C}_6\text{HF}_5$ , and  $\text{C}_6\text{F}_6$ ) at ambient temperature ( $295 \pm 2 \text{ K}$ ). Most previous measurements have been confined to deactivation of  $\text{CO}_2(00^01)$  by small colliders (monatomics and small polyatomics). The deactivation probabilities for the large polyatomic colliders were found to be in the “very high” range and are indicative of intermolecular V–V energy transfer. For example, the value for the deactivation of  $\text{CO}_2(00^01)$  by  $\text{C}_6\text{D}_6$  is ca. 700 times larger than the value for Kr as collider (where

there is no intermolecular V–V transfer). This result is a consequence of the availability of the 30 vibrational modes (and their overtones and combinations) in  $\text{C}_6\text{D}_6$ .

For both  $\text{CO}_2(00^01)$  and  $\text{N}_2\text{O}(00^01)$  there was little difference in the deactivation probabilities between the acyclic ring compounds and their aromatic analogues and the partially fluorinated benzenes but  $\text{C}_6\text{F}_6$  was found to be much less efficient than the other species, probably because its vibrational frequencies are a poor match for those of  $\text{CO}_2$  and  $\text{N}_2\text{O}$ . The perdeuterated species,  $\text{C}_6\text{D}_6$  and  $\text{C}_6\text{D}_5\text{CD}_3$ , especially the latter, showed considerably enhanced deactivation relative to the other species. The results are consistent with V–V deactivation processes dominated by channels with small energy changes and minimal overall change in quantum number. Experiments were carried out with  $\text{C}_6\text{H}_5\text{CD}_3$  and  $\text{C}_6\text{D}_5\text{CH}_3$  as collider gases confirmed that the exceptionally large probabilities for the deactivation of  $\text{N}_2\text{O}(00^01)$  by  $\text{C}_6\text{D}_5\text{CD}_3$  and  $\text{C}_6\text{H}_5\text{CD}_3$  are consistent with domination by near-resonant deactivation to  $\text{N}_2\text{O}(00^00)$  because of the almost exact match between the  $\nu_3$  stretch mode in  $\text{N}_2\text{O}$  at  $2224 \text{ cm}^{-1}$  and the C–D antisymmetric stretch of the methyl group at  $2223 \text{ cm}^{-1}$ .

In contrast to the experiments on deactivation of excited  $\text{CO}_2$  and  $\text{N}_2\text{O}$  by unexcited polyatomics, experiments have been carried out on the deactivation of highly excited polyatomics by triatomics. Early IRF studies using  $\text{CO}_2$  to deactivate azulene<sup>107</sup> and benzene<sup>108</sup> have been enormously extended by the high-resolution tunable diode laser experiments carried out by Flynn and co-workers<sup>44,46,109–112</sup> and by Mullin and co-workers,<sup>47,113–116</sup> which have given considerable insight into the dynamics of energy transfer from highly excited donor molecules to  $\text{CO}_2$ ,  $\text{N}_2\text{O}$ , and  $\text{H}_2\text{O}$ . These two groups have focused on probing the excitation in the bath gas molecules following collision with the hot polyatomic donor molecule (typically, pyrazine and hexafluorobenzene). The experiments yield information on the vibrational and rotational quantum numbers of the scattered bath molecule as well as the distribution of recoil velocities. A significant conclusion arising from the results is that V–V energy transfer is dominated by long-range vibrationally resonant processes, and it displays the characteristic strong inverse temperature dependence. Experimental data on the bath molecule energy gain can also lead to estimates of  $P(E, E')$ . This entails the mapping of bath molecule, state-resolved scattering probabilities into a  $P(E, E')$ .<sup>45</sup> There are limitations, for example, because of the lack of information on energy gain at small  $\Delta E$  ( $< 2000 \text{ cm}^{-1}$ ). However, there is no doubt that data obtained with this technique will be useful in future vibrational energy transfer modeling studies, especially those that consider the energy content in both collision partners before and after a collision.

As a first example of quasiclassical trajectory calculations on the deactivation of a large aromatic molecule by a large polyatomic collider, Lenz and Luther have carried out calculations for highly excited benzene colliding with unexcited benzene.<sup>77</sup> The calculations were carried out for initial energies up to  $40\,700 \text{ cm}^{-1}$  using a LJ potential to describe the interaction between the two benzene molecules. Comparisons were made with the experimental results of Barker et al.<sup>117</sup> from IRF measurements and Nakashima and Yoshihara<sup>118</sup> from UVA measurements. The agreement between the trajectory calculations and experiment is excellent and the energy dependence of the energy transfer predicted by the trajectory calculations is essentially linear. The results of the calculations were divided into the vibrational, rotational, and translational contributions for both the excited molecule and the collider. It was found

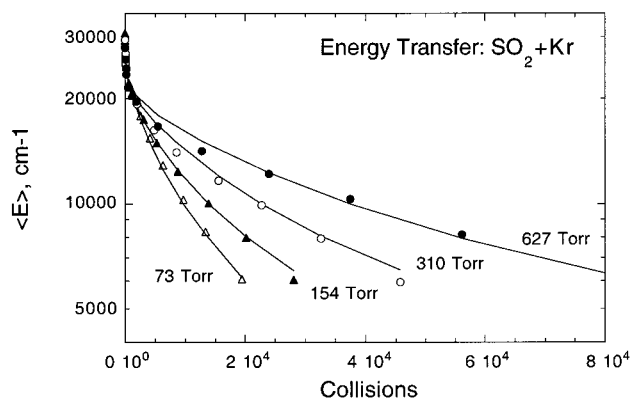


**Figure 4.** Mean vibrational energy vs collisions for SO<sub>2</sub> as a function of pressure.

that V–V energy transfer dominates, it being about a factor of 20 more efficient than V–T energy transfer. Since V–V energy transfer is not well understood at this time, the most practical course of action is to ignore the internal modes of the polyatomic collision partner and adopt large values for  $\langle \Delta E \rangle_d$ , based on tabulations of experimental data.

**Excited Electronic States.** Excited electronic states are important in many chemical systems and they can introduce very complex behavior. The deactivation of NO<sub>2</sub>,<sup>119–121</sup> SO<sub>2</sub>,<sup>122,123</sup> and CS<sub>2</sub><sup>121,123,124</sup> by rare gases exhibits a dramatic increase in energy transfer effectiveness as the internal energy  $\langle E \rangle$  is increased. At low internal energy,  $\langle \Delta E \rangle_{\text{all}}$ , increases roughly quadratically<sup>125</sup> with  $\langle E \rangle$ , but there is a dramatic enhancement at energies in the vicinity of the lowest excited electronic state. Dai et al. proposed that electronic state mixing directly couples the adiabatic electronic states and enhances energy transfer.<sup>126</sup> Recent quantum scattering calculations by Petrongolo and Schatz<sup>127</sup> for He + NO<sub>2</sub> show that vibronic state mixing is required for the energy transfer enhancement and that the enhancement is due to (a) smaller energy gaps between mixed and unmixed states, and (b) resonant energy transfer, when two mixed states contain a common member.

In addition to the enhanced energy transfer near excited electronic state origins,  $\langle \Delta E \rangle_{\text{all}}$  for the deactivation of excited CS<sub>2</sub> and SO<sub>2</sub> by rare gases also exhibits an unusual pressure dependence.<sup>123,124</sup> At high internal energy,  $\langle \Delta E \rangle_{\text{all}}$  is independent of pressure, as expected, but at low internal energy, it takes much larger values at low pressure, as shown in Figure 4. The explanation proposed by Chimbayo et al.<sup>123</sup> for this surprising behavior invokes collision-induced intersystem crossing (CIISC)<sup>128–130</sup> between manifolds of mixed vibronic states of primarily singlet and triplet character, respectively. In the TDTL experiments, the internal energy  $\langle E \rangle$  includes electronic as well as vibrational energy. The pressure dependence of  $\langle \Delta E \rangle_{\text{all}}$  is due to the interplay of collisional VET in each electronic state, combined with the mixed-order pressure dependence of CIISC. At high internal energies,  $\langle \Delta E \rangle_{\text{all}}$  depends mostly on collisional vibrational deactivation, while at low energies it depends mostly on CIISC.

Little information is available from direct experiments concerning average energy transfer quantities for larger molecules in excited electronic states. Weisman and co-workers<sup>131–134</sup> have used a novel technique to deduce the energy transfer parameters for vibrationally excited pyrazine in the triplet state. The results indicate two interesting features: (a) the values for  $\langle \Delta E \rangle$  are much larger than the corresponding values for pyrazine in the ground singlet state and (b) there appears to be a threshold energy below which energy transfer is very inefficient. These

results are provocative, but more experiments are needed to assess whether such effects are of general importance.

**Step-Size Distribution. High Energy.** The IRF and UVA techniques are mostly sensitive to the average energy of the vibrational distribution, although a multiple wavelength version of the IRF method has produced some limited information about the second moment of the evolving distribution during vibrational deactivation.<sup>135</sup> None of these techniques is very sensitive to the detailed shape of the distribution. In contrast, the KCSI technique is very sensitive to the shape of the step-size distribution. The results obtained using several different excited molecules in collisions with several different bath gases show that the step-size distribution for deactivation steps is best described using a generalized version of the exponential model:

$$P(E, E') = \frac{1}{N(E')} \exp\left\{-\left|\frac{E' - E}{\alpha(E')}\right|^\gamma\right\}, \quad \text{for } E' > E \quad (10)$$

where  $N(E')$  is the normalization factor,  $\alpha(E')$  is a linear function of vibrational energy, and  $\gamma$  is a parameter that ranges from  $\sim 0.5$  to  $\sim 1.5$ . When  $\gamma < 1$ , the “wings” of the step-size distribution have enhanced relative probabilities that qualitatively resemble the biexponential distribution. The KCSI results are probably significantly more accurate than the IRF and UVA results; references to published KCSI results are included in Table 1.

**Transition from Low Energy to High Energy.** The state-to-state VET experiments at low energies have clearly revealed dramatic energy transfer propensities, but do these propensities persist at higher vibrational energies? The answer to this question is important for quantitative simulations of energy transfer at low and intermediate energies, such as in shock-induced chemical reactions. Unfortunately, the tools needed to answer the question are not fully developed. State-to-state experimental methods cannot be applied when the states cannot be resolved. Experimental methods that are appropriate for the vibrational quasicontinuum provide only averaged data and cannot determine whether the propensities are present. The VCC-IOS theoretical method is only practical for the lowest energies. Classical trajectories, which already must be used only with caution at high energies, are not appropriate at low vibrational energies. Thus, another approach is needed.

Recently, a modular statistical dynamical theory was described<sup>136,137</sup> that conserves zero-point energy, obeys detailed balance, and employs state-to-state energy transfer models. The aim was to develop a semiquantitative theory that can describe energy transfer over a wide range of state densities. The theory is subject to significant limitations, but the results of the one demonstration calculation carried out thus far are thought-provoking.

The demonstration calculation was for the deactivation of vibrationally excited cyclopropane by helium. The results showed that VET propensities are prominent at low energy, as was found in the state-to-state measurements mentioned above, and are still apparent even at energies where the density of states is  $\sim 10^{10}$  states/cm<sup>-1</sup> (Figure 5). The “smearing out” of the calculated vibrational propensities at higher energies is due to anharmonicity.

The step-size distribution calculated at high densities of states can be represented approximately by the exponential model with parameter  $\alpha(E)$  that is essentially independent of vibrational energy, but an energy-dependent fraction of inelastic collisions. Thus, the *amplitude* of the step-size distribution depends strongly on vibrational energy and gives values for  $\langle \Delta E \rangle_d$  that are proportional to  $E^{3/2}$ . Although this demonstration calculation is

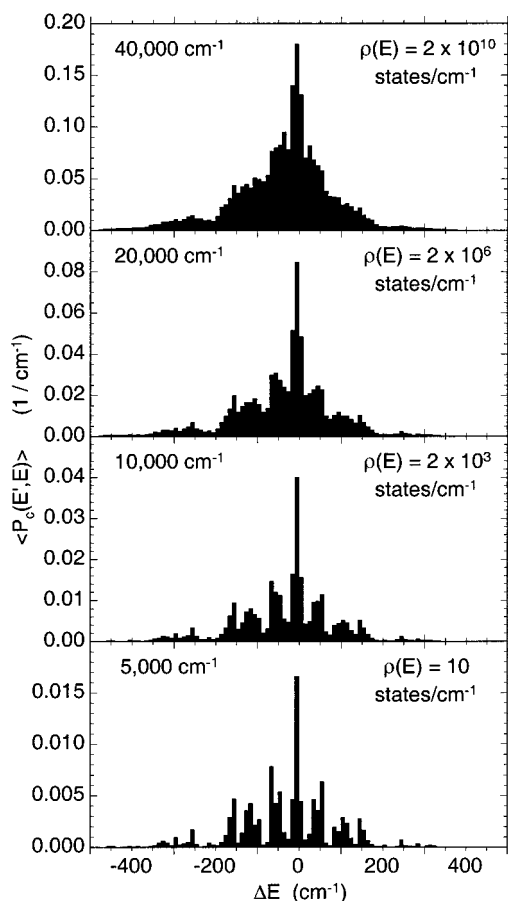


**Figure 5.** Collision step-size distributions at 300 K for cyclopropane deactivation by helium calculated from statistical dynamical theory (see text). The initial excitation energy is given in the upper left corner of each panel.

highly approximate, the variation of the fraction of inelastic collisions with energy is striking, because it calls into question the conventional assumption that all Lennard-Jones collisions are vibrationally inelastic.

The width of the calculated step-size distribution is approximately proportional to temperature, as are the corresponding values for  $\langle \Delta E \rangle_d$ . This result is in general agreement with classical trajectory calculations, but at variance with IRF and UVA experimental data. However, the experimental data analysis was based on the assumption that Lennard-Jones collision frequencies are appropriate. Since  $k_{LJ}$  depends on temperature, a different choice of collision frequency and a reanalysis of the same experimental data could lead to a different conclusion regarding the temperature dependence of  $\langle \Delta E \rangle_d$  and  $\alpha(E)$ . Clearly, much more work is needed to resolve this important problem.

**Recommendations for Modeling.** At vibrational energies below  $\sim 5000 \text{ cm}^{-1}$ , there are only isolated reports of state-to-state energy transfer parameters for polyatomics, and it is not possible to make a general recommendation.

At vibrational energies above  $\sim 5000 \text{ cm}^{-1}$ , the step-size distribution is probably best described by the generalized exponential function (eq 10) with  $\alpha(E)$  depending linearly on vibrational energy. In the absence of specific information, the parameter  $\gamma$  is best assumed to equal unity (exponential model) and the entire function (for deactivation steps) is best assumed to be independent of temperature. The temperature dependence associated with energy transfer will then arise from the activation

collisions (via detailed balance) and from the temperature dependence of  $k_{LJ}$ .

Unless data are to be fitted, values for  $\alpha(E)$  must be estimated. Absolute values for  $\alpha(E)$  have been determined experimentally for only a few species and most of those are aromatics (Table 1). The values for  $\alpha(E)$  for benzene and pyrazine are similar to each other, while those for toluene are significantly larger, probably due to the methyl free rotor. In the absence of other information, values for  $\alpha(E)$  for benzene can be adopted for “stiff” molecules and those for toluene can be adopted for molecules that contain free rotors. This state of affairs is not satisfactory, but there are few alternatives at the present time. Relative and absolute values of  $\langle \Delta E \rangle_d$  reported in many unimolecular reaction studies can be identified with  $\alpha(E_0)$  at the reaction threshold energy ( $E_0$ ). In the absence of additional information, it is reasonable to assume that  $\alpha(E)$  takes the following form:

$$\alpha(E) = c_0 + c_1 E \quad (11)$$

where  $c_0 \approx 40 \text{ cm}^{-1}$  and  $c_1 = (\langle \Delta E \rangle_d - 40)/E_0$ , and  $\langle \Delta E \rangle_d$  corresponds to the reaction threshold. Here, the value for  $c_0$  is a rough average for benzene, toluene, and pyrazine, but note that  $c_0 \approx 0$  for hexafluorobenzene deactivation.

### Modeling of Chemical Systems

Single-channel unimolecular reactions and the corresponding recombination reactions depend critically on VET and “weak collision” models for such systems have been available for decades.<sup>3,10–12</sup> The rate constant falloff in such systems is the principal manifestation of VET. Falloff is a reflection of the fact that the steady-state vibrational energy distribution is deficient in population above the reaction threshold, relative to the equilibrium Boltzmann distribution.<sup>138</sup> This deficiency arises because the VET is not fast enough to activate molecules to energies near and above the reaction threshold and replace those that have reacted: VET becomes the rate-limiting step in the overall process. The modeling of such systems has become routine, although the VET parameters are often not well-known.

The modeling of non-steady-state systems is more demanding. Two examples are given here of non-steady-state systems in which VET is an important factor. Shock tube experiments provide a particularly demanding test of current knowledge of large molecule VET, because both the temperature and vibrational energy distribution vary after passage of the shock. Since VET depends both on bath temperature and on vibrational energy, a considerably detailed model of energy transfer is necessary for a realistic simulation.

Chemical production of vibrationally excited species is a common process in many important systems, including combustion and atmospheric photooxidation. In the second example given here, a nonequilibrium chemical activation system is simulated in which multiple isomerization and fragmentation pathways are present, in addition to VET within each of several potential energy wells. The reaction product yields are highly sensitive to time and pressure, due to VET. This example is used to show the great need for developing the ability to predict energy transfer properties. It also illustrates how a public domain computer program (MultiWell<sup>32</sup>) can be used to model such systems.

**Shock-Induced Chemical Reactions.** The essential features of shock tube experiments have been simulated in several studies.<sup>8,139,140</sup> A nonempirical simulation has not yet been carried out, but the outlines of a possible approach are beginning



to emerge. To construct such a model is a demanding task, because the entire energy range must be dealt with and some of the needed theoretical tools are only poorly developed.

In shock tube experiments, adiabatic compression produces an extremely rapid increase in translational temperature. When a gas is subjected to a sudden adiabatic compression or expansion in a shock wave, momentum and energy are transferred on every collision, and therefore the translational and rotational degrees of freedom equilibrate in a few collisions. The vibrational degrees of freedom, however, transfer energy only slowly. Immediately before the shock, the Boltzmann distribution of vibrational energy is characterized by the initial ambient temperature. After the shock, the vibrational energy increases due to collisions until a new steady-state vibrational distribution is established. The rates of unimolecular reactions, which depend on vibrational (and rotational) energy, are initially very slow, but they increase rapidly as the vibrational energy increases following a shock. Because of the slow vibrational energy transfer, the onset of unimolecular reaction is delayed. The lag time between the shock and the subsequent establishment of a steady unimolecular reaction rate is known as the "incubation time".

Most shock tube experiments are designed so that vibrational relaxation is very rapid and does not interfere with rate constant measurements. Kiefer and co-workers,<sup>141,142</sup> however, have deliberately utilized conditions that permit observation and measurement of both vibrational relaxation and incubation. The most favorable molecules for this purpose are "stiff", with lowest normal mode vibrational frequencies ( $\omega_{\min}$ ) that are relatively high (e.g.,  $\omega_{\min} = 749 \text{ cm}^{-1}$  for cyclopropane). For these molecules, the slowest step in climbing and descending the vibrational energy ladder is the first giant step between the zero level and the next state. If the molecule is diluted in an infinite excess of a monatomic gas, the energy transfer rate is controlled by the slow and inefficient V-T transfer (rotations contribute to this process, as well). The experimental mixtures typically consist of 1%–5% of the reactive gas diluted in a monatomic gas. At these concentrations, collisions between two molecules of the reactive gas are possible and therefore V-V energy transfer, which can be several orders of magnitude faster than V-T energy transfer, may enhance the vibrational relaxation rate.<sup>143</sup>

As explained elsewhere,<sup>8,13</sup> the simulations were carried out using a computer code that employed interpolation of densities of states and other energy-dependent quantities in the quasi-continuum in order to minimize the effects of energy graining and to increase computation speed. The interpolation was carried out by using arrays of data obtained at specific energies (energy grains). At low energies, reliable interpolation is not possible and energy graining is necessary. For these conditions, the computer code used direct numerical integration techniques and only included transitions to and from energy grains that contained states. Thus, the code effectively treated the sparse density of states regime with an energy-grained master equation and it effectively treated the quasicontinuum with a continuum master equation. This hybrid approach (which has also been incorporated in MultiWell<sup>32,34</sup>) is necessary for simulating the entire range of vibrational energy.

Kiefer, Kumaran, and Sundaram<sup>141</sup> (KKS) studied shock-heated norbornene (NB) in Kr bath gas and observed unimolecular dissociation via reaction 12, vibrational relaxation, and incubation over the temperature range from 542–1307 K. KKS used the Schlieren method, which has very good time resolution following the passage of the shock wave. However, the passage

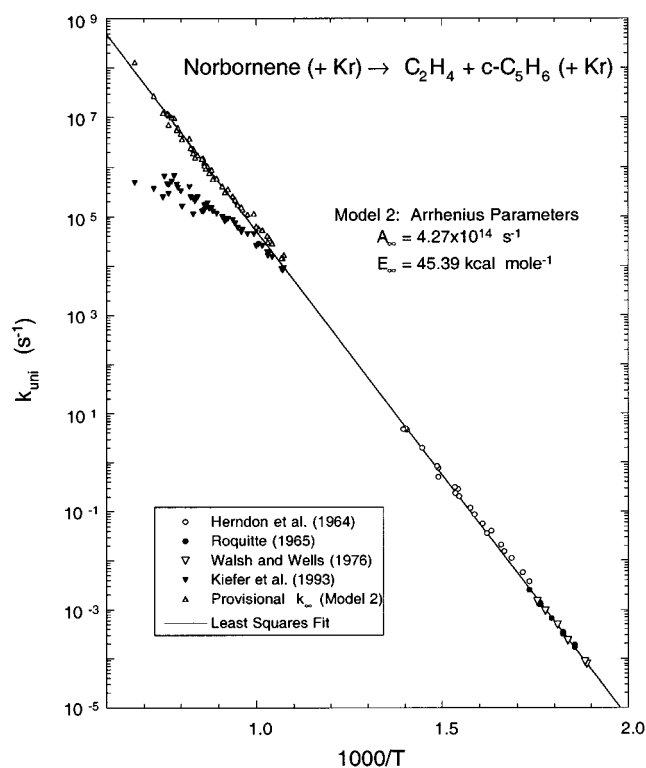
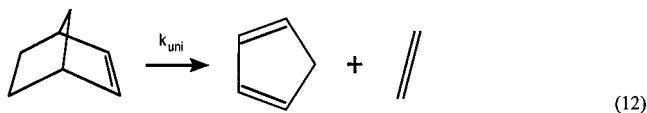


**Figure 6.** Arrhenius plot summarizing experimental data and results from model 2 (the other models show similar good agreement with experiment). The data from Kiefer et al.<sup>141</sup> (KKS) show the effects of falloff. See ref 8 for details.

of the shock wave interferes with the signals at very early times. In a modeling study, Barker and King<sup>8</sup> (BK) combined the KKS rate coefficient data with earlier unimolecular reaction rate data from four previous experimental investigations to cover the temperature range 521–1480 K. The combined data set included rate coefficients ranging over more than 10 orders of magnitude. An Arrhenius plot summarizing all of the experimental reaction rate data is shown in Figure 6. Note that the shock-tube data do not refer to the high-pressure limit except at the low end of the temperature range of these experiments.



BK used a combination of steady-state RRKM calculations and time-dependent master equation calculations to develop a combined energy transfer/reaction model for the simultaneous description of the unimolecular reaction, vibrational relaxation, and incubation data—clearly, a very demanding task for the model. To interpret the incubation time data and extract energy transfer parameters, an accurate RRKM model is needed. To find the RRKM model and microcanonical rate coefficients  $k(E)$ , falloff corrections must be known, but they can only be deduced if the energy transfer parameters are known. Thus, it was necessary to use appropriate assumptions and procedure to arrive at a self-consistent simulation which includes both an RRKM model for  $k(E)$  and energy transfer parameters that are consistent with  $\tau_{\text{inc}}$  and  $\tau_{\text{vib}}$ . Full details are given in the paper by BK.<sup>8</sup> All of the experimental data (incubation times, vibrational relaxation times, and unimolecular rate coefficients) are reasonably consistent with the combined model. Although the NB data set is very extensive, it was still not possible to identify a unique

VET model when both the vibrational relaxation and incubation data were included.

Because only the width of the collision step-size distribution is important in modeling single-channel unimolecular reactions,<sup>12</sup> BK adopted the exponential model and found three empirical expressions for  $\alpha(T, E')$  that are consistent with the entire data set. However, these empirical expressions are merely representative of the unlimited possibilities:

$$\text{model 1: } \alpha_1(T, E') = 10 + 1.1 \times 10^{-5} T E' \quad (13a)$$

$$\text{model 2: } \alpha_2(T, E') = 40 + 5.8 \times 10^{-6} T E' \quad (13b)$$

$$\text{model 3: } \alpha_3(T, E') = 40 + 0.0063 E' \quad (13c)$$

Here, the energies are expressed in  $\text{cm}^{-1}$  units and  $\alpha(T, E')$  is essentially equal to  $\langle \Delta E(E') \rangle_d$ . Note that  $\alpha_3(T, E')$  for model 3 is independent of temperature and is preferred (see Recommendations for Modeling subsection above), but the other two models provide acceptable descriptions of the shock-tube experiments and were used to explore various aspects of the system. It is important to note that experimental uncertainties and the limited temperature and pressure ranges accessible in the shock-tube experiments significantly limit the uniqueness of the resulting models. A further limitation is imposed because the passage of the shock wave obscured the signal at early times: about  $2/3$  of the energy relaxation in each experiment was already complete by the time the vibrational relaxation times could be observed. Because the NB vibrational relaxation time and incubation time data are somewhat redundant and the incubation times are better defined experimentally and are therefore more reliable, the incubation times rather than the vibrational relaxation times were used in the fitting procedure. Thus, BK used the  $\tau_{\text{inc}}$  data in the fitting process and then examined the  $\tau_{\text{vib}}$  data as a test for consistency.

The non-steady-state incubation and vibrational relaxation data are the most important for establishing energy transfer parameters in the NB data set, because the steady-state unimolecular reaction studies (the conventional static and flow system experiments, see Figure 6) were carried out at such high pressures that no falloff was apparent. Had falloff been apparent, it may have provided the best information about VET. The shock tube rate constants do show the effects of falloff, but the pressure range is not large enough and the experimental rate constant uncertainties are not small enough to empirically construct falloff curves. Also, unimolecular reaction rate data were obtained in the experimental shock-tube regime where vibrational relaxation and incubation were too rapid to be observed. A detailed master equation model is necessary.

In a shocked system, the vibrational energy is low initially and VET causes it to increase at a finite rate to a new steady-state value. The sparse density of states regime at low energy is very important, because the large energy gaps between states cause VET to be very slow. The KKS data on vibrational relaxation (without reaction) are somewhat limited and all three models produce acceptable descriptions ( $\pm 30\%$ , based on estimated experimental uncertainties) of the final  $1/3$  of the vibrational relaxation measured in every experiment in the vibrational relaxation data set (see, for example, Figure 7). The three empirical energy transfer models described above give distinctly different steady-state unimolecular reaction rates (Figure 8), but all three models predict incubation times that are consistent with the KKS data, within the estimated  $\pm 30\%$  experimental error and the other limitations of the data set. Since

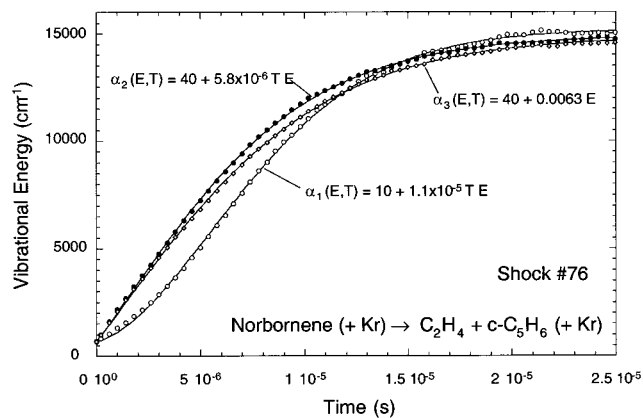


**Figure 7.** Relaxation of average energy as calculated with three energy transfer models for shock no. 76 (KKS).

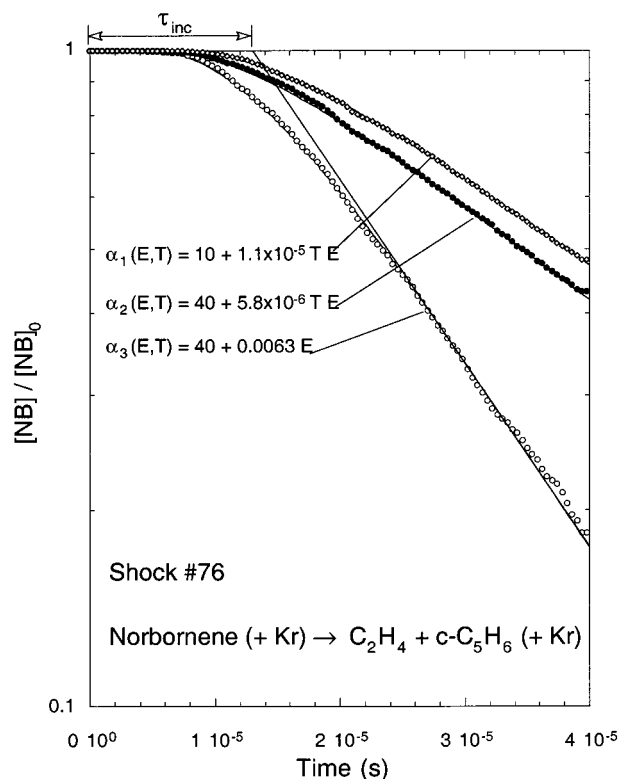


**Figure 8.** Incubation and unimolecular reaction in shock no. 76 (KKS) calculated with three models.

unimolecular reaction rates were not measured in the same experiments as the incubation times, it is not possible to use experimental rate constant data to identify a preferred energy transfer model. Furthermore, systematic variations of a factor of 2–3 in the rate constants predicted by the various energy transfer models can be compensated in the simulations to some extent by systematic changes in the assumed high pressure limit rate coefficients. There is no unambiguous method based solely on the KKS data set for identifying a preferred energy transfer model.

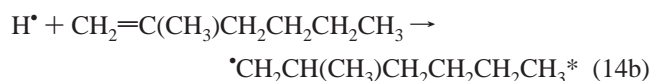
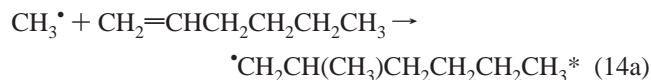
KKS observed that in some systems the rate of energy transfer exhibits a maximum. This finding implies that  $\langle \Delta E \rangle_{\text{all}}$  is small in magnitude at early times, when the average vibrational energy is low, it then increases to a maximum (at intermediate vibrational energies), followed by a decrease as the vibrational relaxation approaches completion (at high average vibrational energies). The results shown for model 1 in Figure 7 exhibit this behavior: the initial slope is relatively small, increases to

a maximum, and then decreases. This behavior is the result of a VET bottleneck at low energies on the vibrational energy ladder. For model 1, this slow rate of energy transfer arises from the small magnitude of  $\alpha_1(T,E)$  and the sparse density of states at low energy. Based on experience gained in modeling this system, it is likely that the maximum in the energy transfer rate can also be produced by using smaller values for  $c_0$  in models 2 and 3. Note, however, that Kiefer and co-workers have concluded that V–V energy transfer may have affected the energy transfer rates at low energies in similar systems.<sup>143</sup>

The shock-tube data for the NB system are too limited to permit identification of a preferred VET model and therefore it was not possible to determine whether the actual  $\alpha(T,E)$  depends on temperature. All three  $\alpha(T,E)$  models depend linearly on vibrational energy. In fact, *no* model that is *independent* of energy was found that can explain the incubation time and vibrational relaxation data while simultaneously fitting the steady-state unimolecular reaction data. Thus, BK concluded that the vibrational energy dependence of  $\alpha(T,E)$  is *required* for modeling unimolecular reaction systems.

An extremely important finding was that the critical energy for reaction deduced from simulating the experiments depends on the specific assumed model for  $\alpha(T,E)$ . This finding has important implications because thermochemical data for transient free radicals are often based on rate constant data that are in the falloff.<sup>144</sup> For the three models described above, the deduced reaction critical energy varied by slightly more than 2 kcal mol<sup>-1</sup>, from which BK concluded that reaction thermochemistry derived from unimolecular reaction rate data in the falloff may vary by a similar amount, depending on the assumed energy transfer model. Since the specific model for  $\alpha(T,E)$  is not known for most reactive species, BK concluded that heats of formation and reaction barrier heights derived from unimolecular reaction studies in the falloff regime may contain an intrinsic uncertainty of several kcal mol<sup>-1</sup>.

**Non-Steady-State Chemical Activation Systems.** In chemical activation, an exothermic chemical reaction produces an excited species which can react further via isomerization and unimolecular decomposition, or be stabilized by collisions.<sup>145–148</sup> For example, the exothermic reactions of atoms and free radicals with olefins produce vibrationally excited free radicals:



where the asterisk denotes vibrational excitation. According to ab initio calculations,<sup>149</sup> the vibrational excitation resulting from reaction 14a is  $\sim 30$  kcal mole<sup>-1</sup>. This excitation energy is considerably greater than the barrier to “tail biting” isomerization, in which the free-radical center abstracts an H-atom from another site on the molecule to produce another 2-methylhexyl free-radical isomer.<sup>150</sup> Chemical activation via reaction 14b is even more exothermic, opening C–H and C–C bond dissociation channels, as well as the isomerization pathways. There are six distinct structural isomers (and several optical isomers) that can interconvert reversibly via three-, four-, five-, six-, and seven-membered ring transition states.<sup>150</sup> In addition, each isomer can decompose via at least two reaction channels (C–H and C–C bond fission).<sup>149</sup> Altogether, there are 14 sets of distinguishable reaction products and 49 reactions.<sup>9</sup> Such a

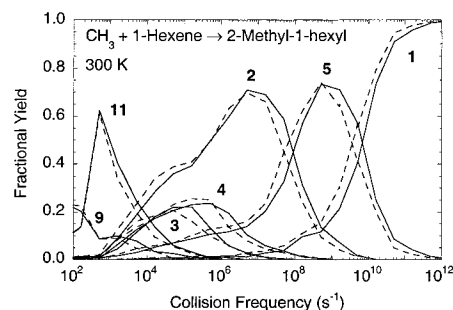


**Figure 9.** Chemical activation product distribution vs collision frequency at 300 K (1 bar of argon). Solid lines, generalized exponential model; dashed lines, exponential model. The numbers in boldface designate isomers according to the free-radical site: “5” designates 2-methyl-5-hexyl radical.

reaction system may seem unusually complicated, but that is not the case. Such reaction networks are common whenever reactions can take place between atoms or free radicals with long-chain unsaturated hydrocarbons, such as in pyrolysis and combustion.

In a recent calculation, the six-isomer 2-methylhexyl radical system was simulated in its entirety using the MultiWell master equation code.<sup>9</sup> Simulations were carried out for shock tube thermal excitation of the radical species, as well as for chemical activation production of excited radicals. Exact counts of states (10 cm<sup>-1</sup> energy grain) were used to calculate RRKM rate constants based on ab initio calculations.<sup>149,150</sup> The isomerization and decomposition product distributions calculated via master equation simulations showed strong similarities for both means of excitation. The simulations required six sets of collisional energy transfer parameters for the six isomers, but *none* are known from experiments. The isomers have different properties, but because they have similar structures and vibrational frequencies, it was assumed that all the isomers have the same Lennard-Jones parameters and collision step-size distributions. Since all of the free radicals contain low frequency torsions, it was assumed that the toluene + argon collision step-size distribution provides a reasonable estimate for the collision parameters, because toluene contains a low-frequency torsion. As pointed out earlier, toluene exhibits more efficient energy transfer than benzene, presumably because of the methyl rotor.<sup>117,151</sup>

Two sets of energy transfer parameters for toluene + argon and were tested: (a) exponential model with parameters from IRF experiments;<sup>117</sup> (b) generalized exponential model with parameters from KCSI experiments.<sup>61</sup> The results for chemical activation simulations are shown in Figure 9 and those for shock tube simulations are shown in Figure 10. For chemical activation via reaction 14a, the final calculated product distributions are shown as a function of collision frequency. It is clear that the two sets of energy transfer parameters give similar results. The similarity is because the two sets are most similar at high vibrational energies and only a few collisions are needed for collisional stabilization to occur. For the shock tube simulations, species concentrations as a function of time are shown in Figure 10. The two energy transfer models give substantially different time dependences, although the general sequence of species appearance and loss are very similar. The different time dependences arise because the differences between the two models are greatest at low energy. The difference accumulates during the many collisions needed for thermal activation.

These results also illustrate the fact that the accuracy required of energy transfer data depends critically on the application: in this case, good simulations can be obtained for the chemical activation system, even if the energy transfer data are inaccurate,

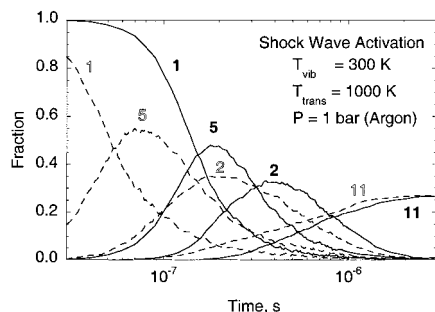


**Figure 10.** Shock-induced fractions vs time at 1 bar of argon and 1000 K. Solid lines and solid numbering: generalized exponential model; dashed lines and open numbering: exponential model. The numbers in boldface designate isomers according to the free-radical site: “5” designates 2-methyl-5-hexyl radical.

but very high quality data are needed to make good estimates of incubation times in shock waves.

## Conclusions

Throughout this paper, we have pointed out what is known, what is not known, and what is currently assumed about energy transfer. We have shown that one can construct reasonable models of realistic chemical systems, despite glaring gaps in knowledge,<sup>1</sup> and we offer convenient “recipes” for modeling, based on current understanding. However, it is very important to recognize the limitations of the models and to work actively on filling the gaps.

Chemistry is entering an age in which accurate computer simulations will become far easier than laboratory experiments. As simulation methods are developed, it is absolutely essential that they be tested through comparisons with experiments. However, experiments on collisional energy transfer are difficult and the process depends on many physical properties. Thus, information about large molecule energy transfer is still fragmentary and unsatisfactory.

The collision step-size distribution  $P(E, E')$  (and its two-dimensional counterpart  $P(E, E'; J, J')$ ) is needed for accurate master equation calculations but it is poorly known both experimentally and theoretically. Much work must be carried out before it will be known with confidence for any system. No direct measurements of  $P(E, E')$  have yet been carried out, although the KCSI technique almost achieves this goal. The functional form of  $P(E, E')$  can be deduced with good confidence from KCSI experiments, but its dependence on temperature is not yet known. New experimental techniques are required, including new experimental approaches which have more specific state preparation and sensitivity. Direct physical measurements are needed on “inaccessible” classes of molecules (e.g., free radicals and alkanes).

Development of reliable models and theories is a high priority, since model calculations do not entail the high cost of time-consuming experiments. Model development requires the answers to many fundamental questions. Is there a clear and accurate correspondence between quantum and classical mechanics which can be exploited? What are the effects of zero-point energy conservation? What are the effects of perturbations and symmetry-breaking? What are the relative contributions of V–T, V–R, and V–V transfer processes? How important are long-range contributions to energy transfer? What are the effects of multiple quantum transitions? How important are the internal, orbital, rotational, vibrational, nuclear spin, and electronic spin forms of angular momentum? Are excited electronic states

different? How are the state-to-state transition probabilities (applicable for the sparse density of states) connected to the  $P(E, E')$  continuum functions needed at high energies? Much work remains to be done on developing models for use in rovibrational (two-dimensional) master equation calculations.

**Acknowledgment.** Financial support at Michigan was provided in part by the US Department of Energy (Office of Basic Energy Sciences) and in part by the donors of the Petroleum Research Fund, administered by the American Chemical Society. Financial support at Adelaide was provided in part by the Australian Research Council. L.M.Y. thanks the Horace H. Rackham School of Graduate Studies for a Predoctoral Fellowship. J.R.B. thanks Prof. William L. Hase and the Chemistry Department at Wayne State University for their hospitality during a sabbatical visit. K.D.K. thanks Adelaide University and the US/Australia Bilateral Science and Technology Program for support of travel in connection with visits to the University of Michigan.

## References and Notes

- (1) King, K. D.; Barker, J. R. “U. S./Australia Workshop on Large Molecule Energy Transfer”, University of Adelaide, 1996.
- (2) Klippenstein, S. J.; Wagner, A. F.; Robertson, S. H.; Dunbar, R.; Wardlaw, D. M. *VariFlex Software*, 1.0 ed.; 1999.
- (3) Tardy, D. C.; Rabinovitch, B. S. *Chem. Rev.* **1977**, *77*, 369.
- (4) Quack, M.; Troe, J. *Spec. Period. Rep.* **1977**, *2*, 174.
- (5) Oref, I.; Tardy, D. C. *Chem. Rev.* **1990**, *90*, 1407.
- (6) Gilbert, R. G. *Int. Rev. Phys. Chem.* **1991**, *10*, 319.
- (7) Flynn, G. W.; Parmenter, C. S.; Wodtke, A. M. *J. Phys. Chem.* **1996**, *100*, 12817.
- (8) Barker, J. R.; King, K. D. *J. Chem. Phys.* **1995**, *103*, 4953.
- (9) Barker, J. R.; Ortiz, N. F. *Int. J. Chem. Kinet.*, in press.
- (10) Robinson, P. J.; Holbrook, K. A. *Unimolecular Reactions*; Wiley-Interscience: New York, 1972.
- (11) Forst, W. *Theory of Unimolecular Reactions*; Academic Press: New York, 1973.
- (12) Gilbert, R. G.; Smith, S. C. *Theory of Unimolecular and Recombination Reactions*; Blackwell Scientific: Oxford, UK, 1990.
- (13) Barker, J. R. *Chem. Phys.* **1983**, *77*, 301.
- (14) Troe, J. *J. Chem. Phys.* **1977**, *66*, 4745.
- (15) Penner, A. P.; Forst, W. *Chem. Phys.* **1976**, *13*, 51.
- (16) Penner, A. P.; Forst, W. *Chem. Phys.* **1976**, *11*, 243.
- (17) Smith, S. C.; Gilbert, R. G. *Int. J. Chem. Kinet.* **1988**, *20*, 307.
- (18) Smith, S. C.; McEwan, M. J.; Gilbert, R. G. *J. Chem. Phys.* **1989**, *90*, 1630.
- (19) Robertson, S. H.; Shushin, A. I.; Wardlaw, D. M. *J. Chem. Phys.* **1993**, *98*, 8673.
- (20) Jeffrey, S. J.; Gates, K. E.; Smith, S. C. *J. Phys. Chem.* **1996**, *100*, 7090.
- (21) Venkatesh, P. K.; Dean, A. M.; Cohen, M. H.; Carr, R. W. *J. Chem. Phys.* **1997**, *107*, 8904.
- (22) Venkatesh, P. K.; Dean, A. M.; Cohen, M. H.; Carr, R. W. *J. Chem. Phys.* **1997**, *111*, 8313.
- (23) Baer, T.; Hase, W. L. *Unimolecular Reaction Dynamics. Theory and Experiments*; Oxford University Press: New York, 1996.
- (24) Perry, D. S. Time scales and mechanisms of intramolecular energy redistribution. In *Highly Excited States: Relaxation, Reaction, and Structure*; Mullin, A., Schatz, G. C., Eds.; American Chemical Society: Washington, DC, 1997; Vol. 678, p 70.
- (25) Lawrance, W. D.; Knight, A. E. W. *J. Chem. Phys.* **1983**, *79*, 6030.
- (26) Stace, A. J.; Murrell, J. N. *J. Chem. Phys.* **1978**, *68*, 3028.
- (27) Yoder, L. M.; Barker, J. R. *J. Phys. Chem. A*, submitted for publication.
- (28) Xue, B.; Han, J.; Dai, H.-L. *Phys. Rev. Lett.* **2000**, *84*, 2606.
- (29) Yardley, J. T. *Introduction to Molecular Energy Transfer*; Academic Press: New York, 1980.
- (30) Durant, J. L.; Kaufmann, F. *Chem. Phys. Lett.* **1987**, *142*, 246.
- (31) Vereecken, L.; Huyberechts, G.; Peeters, J. *J. Chem. Phys.* **1997**, *106*, 6564.
- (32) Barker, J. R. *MultiWell*, 1.01 ed.; <http://aoss.engin.umich.edu/multiwell/>; Ann Arbor, MI, 1999.
- (33) Gilbert, R. G.; Jordan, M. J. T.; Smith, S. C. *UNIMOL Program Suite* Sydney, Australia, 1993.
- (34) Barker, J. R. *Int. J. Chem. Kinet.*, in press.
- (35) Herbst, E.; Dunbar, R. C. *Mon. Not. R. Astron. Soc.* **1991**, *253*, 341.

- (36) Barker, J. R. *J. Phys. Chem.* **1992**, *96*, 7361.
- (37) Brenner, J. D.; Barker, J. R. *Astrophys. J. (Lett.)* **1992**, *388*, L39.
- (38) Barker, J. R.; Brenner, J. D.; Toselli, B. M. The Vibrational Deactivation of Large Molecules by Collisions and by Spontaneous Infrared Emission. In *Vibrational Energy Transfer Involving Large and Small Molecules*; Barker, J. R., Ed.; JAI Press Inc.: Greenwich, CT, 1995; Vol. 2B.
- (39) Golden, D. M.; Rossi, M. J.; Baldwin, A. C.; Barker, J. R. *Acc. Chem. Res.* **1981**, *14*, 56.
- (40) Lupo, D. W.; Quack, M. *Chem. Rev.* **1987**, *87*, 181.
- (41) Bauer, S. H. *J. Phys. Chem.* **1991**, *95*, 6745.
- (42) Oref, I. *J. Chem. Phys.* **1981**, *75*, 131.
- (43) Weston, R. E., Jr.; Flynn, G. W. *Annu. Rev. Phys. Chem.* **1992**, *43*, 559.
- (44) Mullin, A. S.; Park, J.; Chou, J. Z.; Flynn, G. W.; Weston, R. E., Jr. *Chem. Phys.* **1993**, *175*, 52.
- (45) Michaels, C. A.; Flynn, G. W. *J. Chem. Phys.* **1997**, *106*, 3558.
- (46) Flynn, G. W.; Michaels, C. A.; Tapalian, H. C.; Lin, Z.; Sevy, E. T.; Muyskens, M. A. Infrared laser snapshots: Vibrational, rotational, and translational energy probes of high-energy collision dynamics. In *Highly Excited States: Relaxation, Reaction, and Structure*; Mullin, A., Schatz, G. C., Eds.; American Chemical Society: Washington, DC, 1997; Vol. 678, p 134.
- (47) Mullin, A. S.; Schatz, G. C. Dynamics of highly excited states in chemistry: An overview. In *Highly Excited States: Relaxation, Reaction, and Structure*; Mullin, A., Schatz, G. C., Eds.; American Chemical Society: Washington, DC, 1997; Vol. 678, p 2.
- (48) Orr, B. J.; Smith, I. W. M. *J. Phys. Chem.* **1987**, *91*, 6106.
- (49) Krajnovich, D. J.; Parmenter, C. S.; Catlett, D. L., Jr. *Chem. Rev.* **1987**, *87*, 237.
- (50) Mudjijono; Lawrance, W. D. *J. Chem. Phys.* **1998**, *108*, 4877.
- (51) Tanczos, F. I. *J. Chem. Phys.* **1959**, *30*, 1119.
- (52) Schwartz, R. N.; Slawsky, Z. I.; Herzfeld, K. F. *J. Chem. Phys.* **1952**, *20*, 1591.
- (53) Herzfeld, K. F.; Litovitz, T. A. *Absorption and Dispersion of Ultrasonic Waves*; Academic Press: New York, 1959.
- (54) Clary, D. C. *J. Phys. Chem.* **1987**, *91*, 1718.
- (55) Clary, D. C.; Kroes, G. J. Coupled quantum scattering calculations. In *Vibrational Energy Transfer Involving Large and Small Molecules*; Barker, J. R., Ed.; JAI Press Inc.: Greenwich, CT, 1995; Vol. 2A, p 135.
- (56) Clary, D. C.; Gilbert, R. G.; Bernshtein, V.; Oref, I. *Faraday Discussions* **1995**, *102*, 423.
- (57) Smith, G. P.; Barker, J. R. *Chem. Phys. Lett.* **1981**, *78*, 253.
- (58) Hippler, H.; Troe, J.; Wendelken, H. *J. Chem. Phys. Lett.* **1981**, *84*, 257.
- (59) Trevor, P. L.; Rothen, T.; Barker, J. R. *Chem. Phys.* **1982**, *68*, 341.
- (60) Hold, U.; Lenzer, T.; Luther, K.; Reihs, K.; Symonds, A. *Ber. Bunsen-Ges. Phys. Chem.* **1997**, *101*, 552.
- (61) Lenzer, T.; Luther, K.; Reihs, K.; Symonds, A. C. *J. Chem. Phys.* **2000**, *112*, 4090.
- (62) Miller, L. A.; Barker, J. R. *J. Chem. Phys.* **1996**, *105*, 1383.
- (63) Lohmannsroben, H. G.; Luther, K. *Chem. Phys. Lett.* **1988**, *144*, 473.
- (64) Luther, K.; Reihs, K. *Ber. Bunsen-Ges. Phys. Chem.* **1988**, *92*, 442.
- (65) Hold, U.; Lenzer, T.; Luther, K.; Reihs, K.; Symonds, A. C. *J. Chem. Phys.* **2000**, *112*, 4076.
- (66) Fay, N.; Luther, K. *Z. Phys. Chem.* **2000**, *214*, 839.
- (67) Brown, T. C.; King, K. D.; Zellweger, J.-M.; Barker, J. R. *Ber. Bunsen-Ges. Phys. Chem.* **1985**, *89*, 301.
- (68) Zellweger, J.-M.; Brown, T. C.; Barker, J. R. *J. Chem. Phys.* **1985**, *83*, 6251.
- (69) Zellweger, J.-M.; Brown, T. C.; Barker, J. R. *J. Chem. Phys.* **1985**, *83*, 6261.
- (70) Zellweger, J. M.; Brown, T. C.; Barker, J. R. *J. Phys. Chem.* **1986**, *90*, 461.
- (71) Gascooke, J. R.; Alwahabi, Z. T.; King, K. D.; Lawrance, W. D. *J. Chem. Phys.* **1998**, *109*, 3868.
- (72) Gascooke, J. R.; Alwahabi, Z. T.; King, K. D.; Lawrance, W. D. *J. Phys. Chem. A* **1998**, *102*, 8505.
- (73) Ichimura, T.; Mori, Y.; Nakashima, N.; Yoshihara, K. *J. Chem. Phys.* **1985**, *83*, 117–123.
- (74) Damm, M.; Hippler, H.; Olschewski, H. A.; Troe, J.; Willner, J. Z. *Phys. Chem.* **1990**, *166*, 129.
- (75) Barker, J. R.; Golden, R. E. *J. Phys. Chem.* **1984**, *88*, 1012.
- (76) Miller, L. A.; Cook, C. D.; Barker, J. R. *J. Chem. Phys.* **1996**, *105*.
- (77) Lenzer, T.; Luther, K. *J. Chem. Phys.* **1996**, *104*, 3391.
- (78) Grigoleit, U.; Lenzer, T.; Luther, K. *Z. Phys. Chem.* **2000**, *214*, 1065.
- (79) Lin, H.-M.; Seaver, M.; Tang, K. Y.; Knight, A. E. W.; Parmenter, C. S. *J. Chem. Phys.* **1979**, *70*, 5442.
- (80) Heymann, M.; Hippler, H.; Troe, J. *J. Chem. Phys.* **1984**, *80*, 1853.
- (81) Hanning-Lee, M. A.; Green, N. J. B.; Pilling, M. J.; Robertson, S. H. *J. Phys. Chem.* **1993**, *97*, 860.
- (82) Feng, Y.; Niiranen, J. T.; Bencsura, A.; Knyazev, V. D.; Gutman, D.; Tsang, W. *J. Phys. Chem.* **1993**, *97*, 871.
- (83) Knyazev, V. D.; Dubinsky, I. A.; Slagle, I. R.; Gutman, D. *J. Phys. Chem.* **1994**, *98*, 11099.
- (84) Knyazev, V. D.; Dubinsky, I. A.; Slagle, I. R.; Gutman, D. *J. Phys. Chem.* **1994**, *98*, 5279.
- (85) Brown, T. C.; Taylor, J. A.; King, K. D.; Gilbert, R. G. *J. Phys. Chem.* **1983**, *87*, 5214.
- (86) King, K. D. Studies of Collisional Energy Transfer using Pressure-Dependent Very Low-Pressure Pyrolysis (VLPP). In *Advances in Chemical Kinetics and Dynamics. Vol. 2A. Vibrational Energy Transfer Involving Large and Small Molecules*; Barker, J. R., Ed.; JAI Press: Greenwich, CT, 1995; Vol. 2A, pp 171–208.
- (87) Yoder, L. M.; Barker, J. R. Recoil energy distributions in van der Waals cluster vibrational predissociation; ACS Books; 2000.
- (88) Yoder, L. M.; Barker, J. R. *Phys. Chem. Chem. Phys.* **2000**, *2*, 813.
- (89) Brown, N. J.; Miller, J. A. *J. Chem. Phys.* **1984**, *80*, 5568.
- (90) Schranz, H. W.; Troe, J. *J. Phys. Chem.* **1986**, *90*, 6168.
- (91) Whyte, A. R.; Lim, K. F.; Gilbert, R. G.; Hase, W. I. *Chem. Phys. Lett.* **1988**, *152*, 377.
- (92) Schranz, H. W. *J. Mol. Struct.* **1996**, *368*, 119.
- (93) Toselli, B. M.; Barker, J. R. *Chem. Phys. Lett.* **1990**, *174*, 304.
- (94) Oref, I.; Gilbert, R. G. Random walk model for energy transfer at high temperatures. In *Mode Selective Chemistry*; Jortner, J., Levine, R. D., Pullman, B., Eds.; Kluwer Academic Publishers: Dordrecht, The Netherlands, 1991; p 393.
- (95) Schatz, G. C.; Lendvay, G. *J. Chem. Phys.* **1997**, *106*, 3548.
- (96) Miller, W. H.; Hase, W. L.; Darling, C. L. *J. Chem. Phys.* **1989**, *91*, 2863.
- (97) McCormack, D. A.; Lim, K. F. *J. Chem. Phys.* **1997**, *106*, 572.
- (98) Lenzer, T.; Luther, K. *Ber. Bunsen-Ges. Phys. Chem.* **1997**, *101*, 581.
- (99) Lenzer, T.; Luther, K. *J. Chem. Phys.* **1996**, *105*, 10944.
- (100) Yoder, L. M.; Barker, J. R.; Lorenz, K. T.; Chandler, D. W. *Chem. Phys. Lett.* **1999**, *302*, 602.
- (101) Oref, I. Supercollisions. In *Vibrational Energy Transfer Involving Large and Small Molecules*; Barker, J. R., Ed.; JAI Press Inc.: Greenwich, CT, 1995; Vol. 2B, p 285.
- (102) Clarke, D. L.; Oref, I.; Gilbert, R. G.; Lim, K. F. *J. Chem. Phys.* **1992**, *96*, 5983.
- (103) Lim, K. F. *J. Chem. Phys.* **1994**, *101*, 8756.
- (104) Poel, K. L.; Alwahabi, Z. T.; King, K. D. *Chem. Phys.* **1995**, *201*, 263.
- (105) Poel, K. L.; Alwahabi, Z. T.; King, K. D. *J. Chem. Phys.* **1996**, *105*, 1420.
- (106) Poel, K. L.; Glavan, C. M.; Alwahabi, Z. T.; King, K. D. *J. Phys. Chem. A* **1997**, *101*, 5614–5619.
- (107) Barker, J. R.; Rossi, M. J.; Pladziewicz, J. R. *Chem. Phys. Lett.* **1982**, *90*, 99.
- (108) Toselli, B. M.; Barker, J. R. *J. Chem. Phys.* **1991**, *95*, 8108.
- (109) Mullin, A. S.; Michaels, C. A.; Flynn, G. W. *J. Chem. Phys.* **1995**, *102*, 6032.
- (110) Michaels, C. A.; Mullin, A. S.; Flynn, G. W. *J. Chem. Phys.* **1995**, *102*, 6682.
- (111) Michaels, C. A.; Lin, Z.; Mullin, A. S.; Tapalian, H. C.; Flynn, G. W. *J. Chem. Phys.* **1997**, *106*, 7055.
- (112) Michaels, C. A.; Mullin, A. S.; Park, J.; Chou, J. Z.; Flynn, G. W. *J. Chem. Phys.* **1998**, *108*, 2744.
- (113) Fraelich, M.; Elioff, M. S.; Mullin, A. S. *J. Phys. Chem. A* **1998**, *102*, 9761.
- (114) Wall, M. C.; Lemoff, A. S.; Mullin, A. S. *J. Phys. Chem. A* **1998**, *102*, 9101.
- (115) Wall, M. C.; Mullin, A. S. *J. Chem. Phys.* **1998**, *108*, 9658.
- (116) Wall, M. C.; Stewart, B. A.; Mullin, A. S. *J. Chem. Phys.* **1998**, *108*, 6185.
- (117) Barker, J. R.; Toselli, B. M. *Int. Rev. Phys. Chem.* **1993**, *12*, 305.
- (118) Nakashima, N.; Yoshihara, K. *J. Chem. Phys.* **1983**, *79*, 2727.
- (119) Toselli, B. M.; Walunas, T. L.; Barker, J. R. *J. Chem. Phys.* **1990**, *92*, 4793.
- (120) Hartland, G. V.; Qin, D.; Dai, H.-L. *J. Chem. Phys.* **1994**, *100*, 7832.
- (121) Hartland, G. V.; Qin, D.; Dai, H.-L. *J. Chem. Phys.* **1995**, *102*, 8677.
- (122) Qin, D.; Hartland, G. V.; Dai, H.-L.; Chen, C. L. *J. Chem. Phys.* **1996**, *100*.
- (123) Chimbayo, A.; Toselli, B. M.; Barker, J. R. *J. Chem. Phys.* **1998**, *108*, 2383.
- (124) Chimbayo, A.; Toselli, B. M.; Barker, J. R. *Chem. Phys. Lett.* **1996**, *259*, 225.
- (125) Dove, J. E.; Hippler, H.; Troe, J. *J. Chem. Phys.* **1985**, *82*, 1907.

- (126) Dai, H.-L. Collisional energy transfer of highly vibrationally excited molecules: The role of long-range interaction and intramolecular vibronic coupling. In *Highly Excited States: Relaxation, Reaction, and Structure*; Mullin, A., Schatz, G. C., Eds.; American Chemical Society: Washington, DC, 1997; Vol. 678, p 266.
- (127) Petrongolo, C.; Schatz, G. C. *J. Chem. Phys.* **2000**, *112*, 5672.
- (128) Gelbart, W. M.; Freed, K. F. *Chem. Phys. Lett.* **1973**, *18*, 470.
- (129) Freed, K. F. Energy dependence of electronic relaxation processes in polyatomic molecules. In *Radiationless Processes in Molecules and Condensed Phases*; Fong, F. K., Ed.; Springer-Verlag: Berlin, 1976; Vol. 15, p 23.
- (130) Freed, K. F. *Adv. Chem. Phys.* **1981**, *47*, Part 2, 291.
- (131) Bevilacqua, T. J.; Weisman, R. B. *J. Chem. Phys.* **1993**, *98*, 6316.
- (132) McDowell, D. R.; Wu, F.; Weisman, R. B. *J. Phys. Chem.* **1997**, *101*, 5218.
- (133) McDowell, D. R.; Wu, F.; Weisman, R. B. *J. Chem. Phys.* **1998**, *108*, 9404.
- (134) Wu, F.; Weisman, R. B. *J. Chem. Phys.* **1999**, *110*, 5047.
- (135) Brenner, J. D.; Erinjeri, J. P.; Barker, J. R. *Chem. Phys.* **1993**, *175*, 99.
- (136) Barker, J. R. Stalking the Step-size Distribution: A Statistical-Dynamical Theory for Large Molecule Collisional Energy Transfer. In *Highly Excited States: Relaxation, Reaction, and Structure*; Mullin, A., Schatz, G. C., Eds.; American Chemical Society: Washington, DC, 1997; Vol. 678, p 220.
- (137) Barker, J. R. *Ber. Bunsen-Ges. Phys. Chem.* **1997**, *101*, 566.
- (138) Troe, J. *Ber. Bunsen-Ges. Phys. Chem.* **1973**, *77*, 665.
- (139) Dove, J. E.; Troe, J. *Chem. Phys.* **1978**, *35*, 1.
- (140) Shi, J.; Barker, J. R. *Int. J. Chem. Kinet.* **1990**, *22*, 187.
- (141) Kiefer, J. H.; Kumaran, S. S.; Sundaram, S. *J. Chem. Phys.* **1993**, *99*, 3531.
- (142) Fulle, D.; Dib, A.; Kiefer, J. H. *J. Phys. Chem. A* **1998**, *102*, 7480.
- (143) Kiefer, J. H.; Buzyna, L. L.; Dib, A.; Sundaram, S. *J. Chem. Phys.* **2000**, *113*, 48.
- (144) Benson, S. W. *Thermochemical Kinetics*, 2nd ed.; Wiley: New York, 1976.
- (145) Larson, C. W.; Rabinovitch, B. S.; Tardy, D. C. *J. Chem. Phys.* **1967**, *47*, 4570.
- (146) Larson, C. W.; Chua, P. T.; Rabinovitch, B. S. *J. Phys. Chem.* **1972**, *76*, 2507.
- (147) Carter, W. P. L.; Tardy, D. C. *J. Phys. Chem.* **1974**, *78*, 2201.
- (148) Malins, R. J.; Tardy, D. C. *Int. J. Chem. Kinet.* **1979**, *11*, 1007.
- (149) Yamauchi, N.; Miyoshi, A.; Kosaka, K. *J. Phys. Chem. A* **1999**, *103*, 2723.
- (150) Viskolcz, B.; Lendvay, G.; Seres, L. *J. Phys. Chem. A* **1997**, *101*, 7119.
- (151) Linhananta, A.; Lim, K. F. *Phys. Chem. Chem. Phys.* **1999**, *1*, 3467.
- (152) Shi, J.; Barker, J. R. *J. Chem. Phys.* **1988**, *88*, 6219.
- (153) Hippler, H.; Otto, B.; Troe, J. *Ber. Bunsen-Ges. Phys. Chem.* **1989**, *93*, 428.
- (154) Hippler, H.; Troe, J.; Wendelken, H. J. *J. Chem. Phys.* **1983**, *78*, 5351.
- (155) Hippler, H.; Troe, J. Recent direct studies of collisional energy transfer on vibrationally excited molecules in the electronic ground state. In *Advances in Gas-Phase Photochemistry and Kinetics: Bimolecular Collisions*; Ashfold, M. N. R., Baggott, J. E., Eds.; The Royal Society of Chemistry: London, 1989; p 209.